Reaction Chemistry & Engineering

ROYAL SOCIETY OF CHEMISTRY

PAPER

View Article Online
View Journal

Cite this: DOI: 10.1039/d6re00057f

Low-temperature standard-SCR over Cu-SSZ-13: selective inhibition of the oxidation half-cycle by mild hydrothermal aging

Andrea Gjetja, [a] Nicola Usberti,[a] Nicole Daniela Nasello,[a] Umberto Iacobone,[a] Isabella Nova, [a] Enrico Tronconi, *[a] Rohil Daya, [b] Lai Wei,[b] Hongmei An[b] and Krishna Kamasamudram[b]

Received 18th February 2026,
Accepted 6th April 2026

DOI: 10.1039/d6re00057f

rsc.li/reaction-engineering

The impact of mild hydrothermal aging (HTA) on low-temperature (150–200 °C) standard-SCR is investigated using transient response methods and transient kinetic analysis. We decouple the reduction and the oxidation half-cycles (RHC and OHC) of the standard-SCR redox mechanism to study them independently. While the RHC rates are essentially unaffected, OHC is inhibited by mild HTA. By equating the estimated rate expressions (both 2nd order in Cu sites, OHC with O_2 as the sole oxidant), we predict exactly the steady-state low-temperature standard-SCR performance in terms of both NO conversion and bed-average Cu redox state, as well as the detrimental effect of mild HTA on the DeNOx efficiency. We also demonstrate that the DeNOx activity of the aged catalyst can be precisely restored by incrementing the oxygen partial pressure in proportion to the drop of the OHC rate constant, as predicted by our simple two-reaction model. These findings offer valuable insights into the design of next-generation urea-SCR exhaust gas aftertreatment (EGA) systems featuring enhanced cold-start performance and durability under aging conditions.

1. Introduction

Nitrogen oxides (NOx) in diesel engine vehicles' exhausts – both light- and heavy-duty – remain a critical challenge for human health and the environment.[1,2] In this context, maintaining high deNOx performance at low temperatures is particularly important, since the SCR catalyst is often required to operate during cold-start and other low-load driving conditions, where hydrothermal aging can further deteriorate activity.[3,4] This leads to a continuous interest in ammonia-selective catalytic reduction (NH_3-SCR), a well-established technology, which reduces NOx to harmless N_2 through the use of aqueous urea.[5,6] The main reactions are the standard-SCR, where NO, NH_3, and O_2 are combined (R1), and fast-SCR (R2), involving NO_2.

$$2NO + 2NH_3 + 1/2O_2 \rightarrow 2N_2 + 3H_2O \quad (R1)$$

$$NO + 2NH_3 + NO_2 \rightarrow 2N_2 + 3H_2O \quad (R2)$$

The state-of-the-art SCR catalysts for mobile applications are metals-exchanged zeolites, in particular copper-chabazite, a small-pore type zeolite, such as Cu-SSZ-13.[7] They are characterized by high selectivity to nitrogen, a wide operating temperature range, and hydrothermal stability.[7–9] Copper-exchanged zeolites are usually preferred to iron-zeolites due to their higher low-temperature activity ($T \leq 250$ °C)[10] even in the absence of NO_2 (produced by the upstream diesel oxidation catalyst, DOC), which is necessary for fast-SCR to occur (R2).

It is well-established that standard-SCR works with a Cu/redox mechanism at low temperatures,[11–15] composed of reduction and oxidation half-cycles (RHC and OHC, respectively), where isolated copper ions cycle between Cu^{2+} and Cu^{+}. Recent works[14–18] demonstrated the low-T reaction stoichiometries for RHC and OHC (reported as (R3) and (R4)); summed, they lead to the standard-SCR reaction (R1).

$$2Cu^{2+}OH(NH_3)_3 + 2NO \rightarrow 2Cu^{+}(NH_3)_2 + 2N_2 + 4H_2O \quad (R3)$$

$$2Cu^{+}(NH_3)_2 + H_2O + 1/2O_2 + 2NH_3 \rightarrow 2Cu^{2+}OH(NH_3)_3 \quad (R4)$$

The RHC is characterized by an equimolar consumption of NO and NH_3, production of nitrogen, and Cu^{2+} reduction to Cu^{1+} ($NO : NH_3 : Cu^{2+} = 1:1:1$), involving two-proximate

[a] Laboratory of Catalysis and Catalytic Processes, Dipartimento di Energia, Politecnico di Milano, Via La Masa, 34, Milan, 20156, Italy.
E-mail: enrico.tronconi@polimi.it; Tel: +39 02 2399 3264
[b] Cummins Inc., 1900 McKinley Avenue, Columbus, Indiana 47201, USA

ammonia-solvated Cu ions.[14,19–22] The OHC (R4) works in the presence of sole oxygen and is promoted by water that acts as a proton transfer molecule, as recently confirmed through DFT calculations by Contaldo *et al.*:[23] O_2 is activated by two diamino Cu^+ complexes $Cu^+(NH_3)_2$ to form a μ-oxo Cu^{2+}-dimer $Cu_2{}^{2+}(NH_3)_4O_2$, while H_2O is oxidized to H_2O_2, which acts as an oxygen shuttle to oxidize an additional pair of $Cu^+(NH_3)_2$.

Notice that reactions (R3) and (R4) rely on NH_3-solvated mobile $Cu^{2+}OH$ moieties, originating from $ZCu^{2+}OH$ framework-bound species, but the SCR-active sites precursors also include the bidentate Z_2Cu^{2+} species (Z is the AlO_4^- of the zeolite framework), which are also thermodynamically favored. The Cu speciation, in fact, depends on the catalyst formulation[24] (*i.e.*, on the Si/Al and the Cu/Al ratios) and/or on the extent of aging.[25–27] Indeed, because the upstream DOC and diesel particulate filter (DPF) generate exothermic reactions during hydrocarbon and soot oxidation, the downstream NH_3-SCR catalyst is exposed to higher temperatures in the presence of water and oxygen.[28,29] If the temperature is limited to 600–700 °C, it results in mild hydrothermal Aging (HTA) of the catalyst: the dealumination of the zeolite is minimal in these conditions.[30,31] Instead, during mild HTA, the Cu speciation is shifted, with a combination of the single-bonded copper atoms with a Brønsted acid site (BAS) to form the double-bonded copper atom:

$$ZCu^{2+}OH + ZH^+ \rightarrow Z_2Cu^{2+} + H_2O \quad \text{(R5)}$$

Different methods have been used to quantify this phenomenon (*e.g.*, NH_3 titration,[32] NO_2 desorption,[33] H_2-TPR,[34] EPR[25]), but a correlation with the loss of performance of the SCR catalyst is still difficult to identify. Indeed, it is known that over Cu-SSZ-13 NO conversion slightly decreases under mild HTA,[8,9,25] but a correlation with the shift in copper speciation remains to be established, to our knowledge. Wenig *et al.*[35] have combined steady-state standard-SCR data and *Operando* XAS over Cu-CHA and Cu-AEI: at low *T*, they report a drop of the oxidized copper fraction during standard-SCR with HTA, *e.g.*, at 150 °C over Cu-CHA from ~30 to 0%. Zhang *et al.*[36] have prepared samples with different Cu speciation ($ZCu^{2+}OH$ fraction from 73 to 86%), and have seen that, with HTA, the catalyst with the lowest $ZCu^{2+}OH$ had the lowest loss of performance. Deka *et al.*[37] have shown how classical mild HTA slightly worsens the DeNOx performances at low *T*, and mild HTA in H_2-ICE conditions (high water content and/or H_2 slip presence) further decreases the performances. Experimental and modeling work from Zheleznyak *et al.*[38] has indicated that Z_2Cu^{2+} sites are inactive in NO oxidation.

Additionally, the effect of mild HTA on the two half-cycles of the redox mechanism (RHC and OHC) has been studied under different conditions. Gramigni *et al.*,[20] Daya *et al.*,[17] and Nasello *et al.*[39] have all demonstrated that the RHC over different-aged Cu-CHA catalysts with diverse Cu loadings and SAR is hardly affected by mild HTA up to 350 °C, both in dry and wet conditions. This is possibly due to the hydrolysis reaction – *i.e.*, (R5) reverse –, which is not kinetically limited when the RHC is taking place, as shown by DFT calculations by Hu *et al.*[40] Deka *et al.*[41] have investigated a field-aged catalyst at high temperatures: while confirming that aging does not have an impact on RHC, they show instead that the OHC is greatly affected. The activation energy of the standard-SCR of the degreened sample is shown to be between the RHC and the OHC activation energies, while for the field-aged, the standard-SCR E_A was almost equal to the E_A of the OHC only, suggesting its role as the rate determining step (RDS).

In this work, we focus on how mild HTA affects both the RHC and the OHC, coupling transient tests in laboratory-controlled conditions with kinetic analysis. This will allow us, using transient response methods and a simple two-reaction model, to predict the behavior of the catalyst and its performance during mild HTA. Also, we propose a methodology to recover the activity over the aged catalyst based on the findings reported here and in previous works.

2. Materials and methods

2.1. Experimental set-up

The experiments are conducted over two Cu-SSZ-13 samples with the same copper loading (2.6% w/w) and silica-to-alumina ratio (SAR, equal to 30), both quantified by ICP-MS. The two samples were provided by Cummins Inc. in the form of washcoated honeycomb monoliths; catalytic powders were scratched from the monolith, characterized by ICP analysis and loaded in the test reactor.

The first sample was conditioned at 550 °C for four hours at 10% v/v of both H_2O and O_2 in N_2. Conversely, the second sample went through a mild hydrothermal aging protocol: 650 °C for 50 h under the same inlet gas conditions. In the following, the two samples will be called degreened and aged (shortened to deg and aged in the figures).

In the kinetic experiments, two quartz tubular reactors (ID = 6 mm) are loaded with 32 mg of catalyst powders diluted with 98 mg of cordierite powders. Both the samples and the cordierite are sieved to 140–200 mesh to avoid internal mass transfer limitations. The overall load of Cu in the reactor is 13.0 μmol in all the experiments. A thermocouple (K-type) is placed on top of the catalyst bed, assuring correct contact between the two, and is used to control the electric furnace to set the reactor temperature. The reactor has three feed lines: a main one with He and two lines connected to six-way valves. These valves are used to step feed and remove the main gas species. Indeed, by a simple switch, we are able to feed NO, NO_2, NH_3, and/or O_2; when not needed, we feed helium at the same flow rate. The main line of helium can be switched to a saturator in order to have water vapor in the line. The reactor outlet line is split into two online gas analyzers: a UV analyzer (ABB Limas 11HW) and a mass spectrometer (Hiden QGA). The first is used to measure the

NO, NO_2, and NH_3, while the second measures N_2, Ar (used as pulse-valve tracer), O_2, and H_2O concentrations. All the lines are heated at 180 °C to prevent water condensation and/or ammonium nitrate formation.

2.2. Experimental procedures

The transient response methods (TRMs) used in this work resemble those of our recent works.[16,39] A quick recap of the procedures is reported here with details on the specific experimental conditions:

– NO_2 adsorption + TPD: after a pre-oxidation of the catalyst at 550 °C with 8.0% v/v of O_2 in He, the temperature is set to 150 °C and 500 ppm of NO_2 in He are fed to the reactor. The GHSV is set to 266 250 $cm^3\ h^{-1}\ g_{cat}^{-1}$ (STP). Nitrates are formed and stored on the catalyst *via* disproportionation of NO_2 with the formation of NO.[42,43] After a purge in He, the catalyst undergoes a Temperature-Programmed Desorption (TPD) up to 550 °C with a heating rate of 15 °C min^{-1}. This protocol is used to evaluate the copper speciation ($ZCu^{2+}OH$ and Z_2Cu^{2+}) by assuming that the $ZCu^{2+}OH$ fraction is equal to the ratio of the NO_2 released upon nitrates decomposition during the TPD to the total reducible Cu present in the sample.[44]

– Reduction half-cycle: the catalyst is pre-oxidized at 550 °C with 8.0% v/v of O_2 in He for 1 h, followed by cooling to the desired temperature (150, 175, or 200 °C). The GHSV is set to 450 000 $cm^3\ h^{-1}\ g_{cat}^{-1}$ (STP). Once the test temperature is reached, we inject 2.0% v/v of H_2O *via* the saturator if the experiment is in wet feed conditions. Then we also feed 500 ppm of NH_3 in He until reaching full saturation of the catalyst, to decouple the RHC from the NH_3 adsorption on the catalyst.[14,20,21] As soon as the catalyst is fully saturated, NO (500 ppm) is added to monitor the transient consumption (and the associated nitrogen production) and, thus, the RHC dynamics under isothermal conditions. We also calculate the amounts of NO consumed and N_2 produced by integrating the outlet concentration traces over time.

– Oxidation half-cycle: the catalyst is fully reduced with 500 ppm of NO, 500 ppm of NH_3, and 2% of H_2O in He and then oxidized with 1.0% v/v of O_2 and 2.0% of H_2O in He. Like for the RHC tests, the GHSV is equal to 450 000 $cm^3\ h^{-1}\ g_{cat}^{-1}$ (STP). The process is continuously repeated by changing the duration of the oxidation step (*e.g.*, 1 min, 7 min, 1 h, *etc.*), to assess the temporal evolution of the oxidized copper fraction.[16] By integrating the amount of NO consumed and N_2 produced during the reduction step, which follows each oxidation at different times, and exploiting the $Cu^{2+}:NO:N_2 = 1:1:1$ molar ratios, the Cu^{2+} fraction is computed as in eqn (1):

$$\sigma = \frac{Cu^{2+}}{Cu_{tot}} = \frac{\text{mean}\left(n_{NO}^{cons}, n_{N_2}^{prod}\right)}{n_{Cu_{tot}}} \quad (1)$$

– Standard-SCR: after pre-reduction with 500 ppm of NO, 500 ppm of NH_3, and 0.0–2.0% v/v of H_2O in He, 8.0% v/v of O_2 is added to the NO + NH_3 feed stream to start the standard-SCR activity; conditions are kept stable to ensure steady-state NO conversion. After two hours, we shut off oxygen to induce a final NO + NH_3 reduction step and, thus, quantify the bed-average Cu oxidized fraction reached under steady-state standard-SCR conditions. The procedure is described in detail by Nasello *et al.*[16] Additional tests were performed feeding 4.0 and 5.8% of O_2 during standard-SCR.

2.3. Transient kinetic analysis

The transient kinetic analysis (TKA) of the RHC, OHC, and standard-SCR data is the same as that applied in recent publications.[16,39] The plug flow test reactor is modelled as a series of 20 isobaric and isothermal CSTRs, each of them associated with a transient mass balance equation in Cu^{2+}, NO, and N_2, as previously reported.[16] The RHC rate equation, as in eqn (2), is written assuming first order kinetics in NO, zeroth order in NH_3 (due to catalyst saturation), and second order in the oxidized copper fraction (σ).[17,20,21] Instead, for the OHC rate, eqn (3), we assume first order in O_2, zeroth order in NO, and second order in the reduced copper fraction $(1-\sigma)$.[16,17] A first order in $(1-\sigma)$ is also used to further prove that is not consistent in low T OHC. In eqn (2) and (3), y_{NO}^{ref} and $y_{O_2}^{ref}$ are the reference concentration for NO and O_2, set to 500 ppm and 8.0% v/v, respectively.

$$r_{RHC} = k_{RHC}\frac{y_{NO}}{y_{NO}^{ref}}\sigma^2 \quad (2)$$

$$r_{OHC} = k_{OHC}\frac{y_{O_2}}{y_{O_2}^{ref}}(1-\sigma)^2 \quad (3)$$

Normalization of the rate constants by the reference NO and O_2 mole fractions makes the rate constants equal to TORs at reference conditions, thus facilitating the comparison of the RHC and OHC rates.

It is worth mentioning that the effects of H_2O concentration and NH_3 solvation of Cu^{II} sites are herein lumped in the two rate constants k_{RHC} and k_{OHC}. While the effect of H_2O feed contents will be assessed directly by carrying out tests under both wet (H_2O = 2% v/v) and dry (H_2O = 0% v/v) feed-gas conditions, the effects of ammonia concentration and Cu solvation are not investigated in this work. Nevertheless, Usberti *et al.*[45] demonstrated in a recent publication that, if the catalyst is fully saturated with NH_3, Cu^{2+} reduction transients (RHC) are essentially unaffected by changing the gas-phase ammonia concentration. On the contrary, inhibition of the low-temperature standard-SCR activity was observed when increasing the NH_3/NO feed ratio from 1 to 1.5 and 2; accordingly, this effect was ascribed to ammonia inhibition of the sole OHC. In this paper, in order to assess the effect of the catalyst aging, the OHC will be investigated independently by dedicated transient tests.

3. Results and discussion

3.1. Effect of mild HTA on Cu speciation and NO conversion

The NO_2 adsorption + TPD experimental protocol is applied to the degreened and aged samples to assess their Cu^{2+} speciation. Results are reported in the SI as Fig. SI.1.

During the TPD, the degreened and the aged samples released 10.4 and 4.9 μmol of NO_2, which correspond to a $ZCu^{2+}OH$ fraction of 80.0 and 37.7%, respectively. As previously stated, mild HTA reduces the amount of $ZCu^{2+}OH$, converting them into double-bonded Z_2Cu^{2+} sites.[33] These values are in line with experimental and modeling work from Daya *et al.*,[27] where they used NH_3 adsorption + TPD for the characterization, and from Iacobone *et al.*[33]

The NO conversion during steady-state standard-SCR at 150, 175, and 200 °C over the degreened and aged samples is plotted in Fig. 1. As anticipated in the Introduction, mild HTA results in a measurable loss of DeNOx activity across the entire temperature range studied. Specifically, the NO conversion drops from 33.7 to 24.9% at 150 °C, and from 75.9 to 68.8% at 200 °C. This motivates the subsequent investigation of the two half-cycles of the redox mechanism (RHC and OHC) with the goal of identifying which is responsible for the observed activity loss.

3.2. Effect of mild HTA on low-*T* RHC

In a recent work,[39] we explored the effect of Mild HTA on the reduction-half cycle in a wider temperature range (135–350 °C), both in dry and wet feed conditions. We have confirmed the marginal effect of hydrothermal aging on the Cu reduction rate, the inhibition due to the presence of water, and that a rate expression second order in the oxidized copper fraction, as seen in eqn (2), accurately predicts the transient dynamics.

In this work, we run the same experiments on this new set of catalysts, focusing on the 150–200 °C range in wet conditions (H_2O = 2.0% v/v). The empty symbols in Fig. 2 show the experimental data collected during the reduction half-cycle protocol applied to the degreened (panels A, B, C) and to the aged samples (panels D, E, F), at three temperatures.

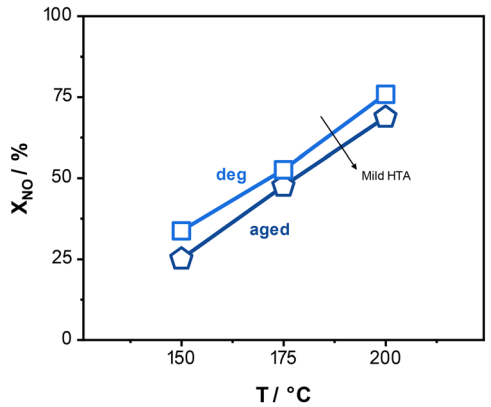

Fig. 1 NO conversion during the standard-SCR protocol on degreened and aged catalysts at 150, 175, and 200 °C. Symbols: squares for degreened, pentagons for aged sample. Feed: GHSV = 450 000 $cm^3\ h^{-1}\ g_{cat}^{-1}$ (STP); NO = 500 ppm, NH_3 = 500 ppm, O_2 = 8.0% v/v and H_2O = 2.0% v/v in He.

When a step feed of 500 ppm of NO and 500 ppm of NH_3 is fed to a pre-oxidized NH_3-saturated sample, a N_2 peak is produced while NO is consumed. As the catalyst approaches full reduction, NO approaches the feed concentration value, while N_2 is no longer produced. These dynamics become faster by progressively increasing temperature: a positive effect of temperature on the reduction process is apparent, as NO and N_2 concentrations approach their asymptotic levels faster (approximately 800, 600, and 400 s, respectively, for 150, 175, and 200 °C).

Comparing data obtained over the two samples (for clarity, Fig. SI.2 of the SI shows the superimpositions of the experimental data), the negligible effect of mild HTA on the RHC transients is clearly apparent across the 150–200 °C range. Table SI.1 reports the integral values of NO converted and N_2 released in the different experiments, which are slightly lower than the total amount of copper present in the reactor. This could be associated with two different aspects: i) the catalyst not being fully oxidized at t = 0 s of the transients due to ammonia oxidation during the pre-treatment (when NH_3 + O_2 are fed to pre-oxidize and saturate the catalyst); ii) part of the Cu in the catalysts can be present as Cu oxides (namely, CuOx) and not involved in the redox cycle. This last explanation is in line with Yao and coworkers,[46] who reported a significant CuOx content for samples with high Cu loading (≥2.0% w/w).

In agreement with recent publications,[39] transient kinetic analysis of the data in Fig. 2 provides a quantitative evaluation of the RHC rate. In Fig. 2, the solid lines for NO and N_2 illustrate the model fit obtained with these rate constants. Table 1 shows the respective rate constants estimated by the experimental data fit over the two samples at different temperatures.

In line with the previous discussion, the rate constants increase with increasing temperature and are almost identical between the two samples. Fig. SI.3 shows the corresponding Arrhenius plots: the estimated activation energy of the degreened is 27.7 kJ mol^{-1}, while for the aged catalyst it is 29.1 kJ mol^{-1}. As expected, the two E_A are similar since no promotion or inhibition by mild HTA is observed on RHC. This can be explained by the occurrence of the hydrolysis reaction:[40] Z_2Cu^{2+} sites are converted back to $ZCu^{2+}OH$ at a rate faster than the RHC and, thus, not kinetically relevant. These findings clearly indicate that RHC cannot be considered responsible for the low-temperature activity loss associated with the aging process.

3.3. Effect of mild HTA on low-*T* OHC

A novelty of this work lies in addressing the effect of mild HTA on the low-temperature oxidation half-cycle. Fig. 3 shows the experimental data (empty symbols)

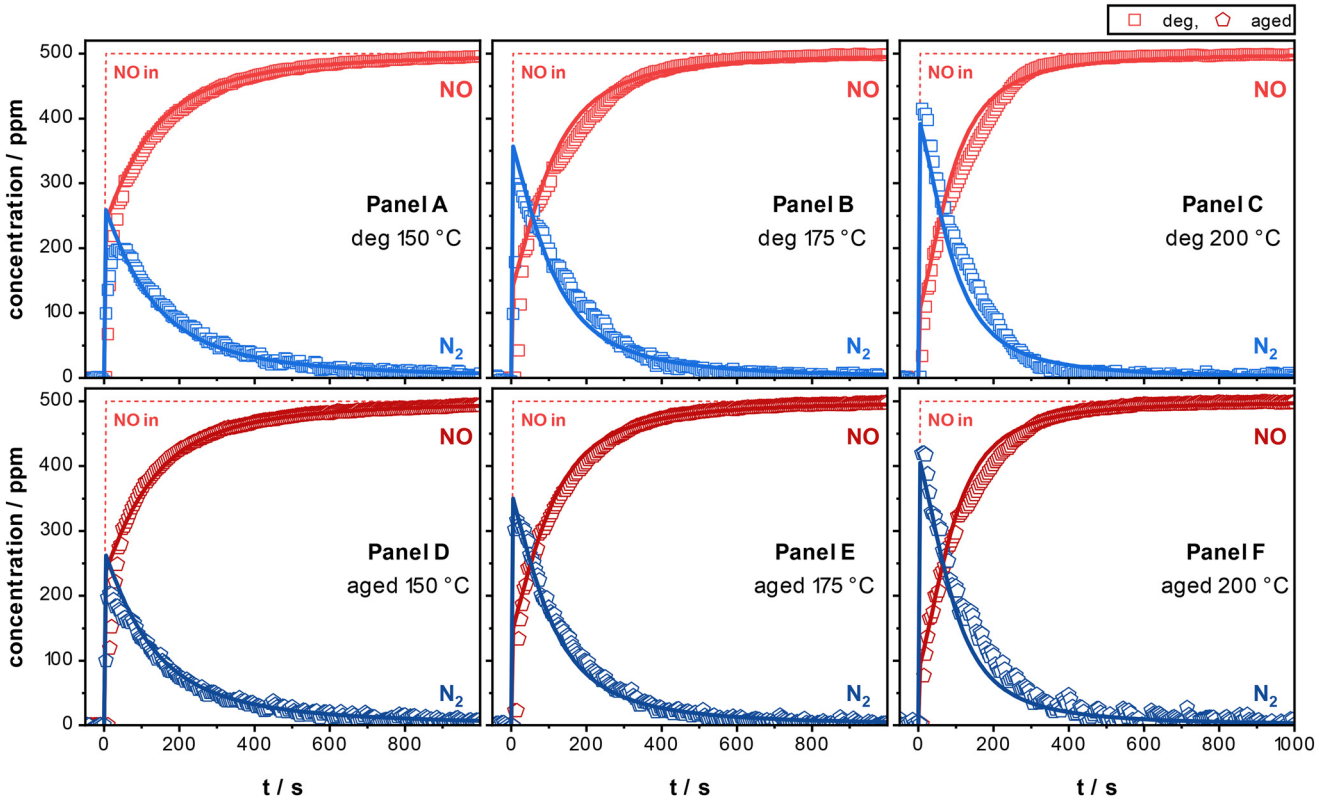

Fig. 2 NO and N_2 dynamics during the RHC protocol on degreened and aged samples. Panels: A) deg 150 °C, B) deg 175 °C, C) deg 200 °C, D) aged 150 °C, E) aged 175 °C, F) aged 200 °C. Symbols: experimental data (red for NO, blue for N_2, squares for deg, pentagons for aged). Solid lines: model fit. Feed: GHSV = 450 000 $cm^3\ h^{-1}\ g_{cat}^{-1}$ (STP); NO = 500 ppm, NH_3 = 500 ppm and H_2O = 2.0% v/v in He.

collected with the OHC protocol over the degreened (panels A, B, C) and over the aged (panels D, E, F) samples at 150, 175, and 200 °C.

As shown in Fig. 3, the longer the oxygen exposure time, the higher the catalyst oxidation extent. Full oxidation is approached only over the degreened sample at 200 °C, after 1 h, due to the low O_2 partial pressure employed in these tests. The 1.0% v/v concentration of oxygen is chosen specifically for the purpose of slowing down the OHC to improve the evaluation of the respective rate constant. Indeed, we have previously assessed[16] the linear dependence of the OHC rate on the oxygen concentration. Increasing the temperature, we observe a faster oxidation of the Cu sites, in line with previous findings on different catalysts.[16]

Comparing the data for the two samples (the experimental dataset at 150 °C is available in Table SI.2), we can see that the oxidation of the aged sample is always slower than the degreened across the whole set of investigated temperatures.

Table 1 RHC rate constants over the degreened and the aged samples at the three studied temperatures

k_{RHC}/s^{-1}	Degreened	Aged
150 °C	4.6×10^{-3}	4.3×10^{-3}
175 °C	6.7×10^{-3}	6.9×10^{-3}
200 °C	10.6×10^{-3}	10.3×10^{-3}

When coupled with the almost negligible HTA effect detected for the RHC, this result ascribes the typical deNOx performance loss following mild HTA to the inhibition of the OHC only. This will be further discussed and supported in section 3.4, where we combine RHC and OHC into the overall standard-SCR reaction.

Eventually, TKA is applied to the OHC experiments in Fig. 3, fitting the second order OHC rate model (eqn (3)) to the data and estimating the rate constants. Table 2 lists the k_{OHC} estimates, and the solid lines in Fig. 3 show the respective transient fit. Just as a comparison, the gray dashed lines show instead the fit assuming a 1st order in reduced Cu in the r_{OHC}. As previously assessed,[16] the quality of the fit is much worse, confirming the validity of the second order OHC kinetics.

In agreement with the previous discussion, the k_{OHC} estimates are consistently smaller over the aged sample, while a positive temperature effect is observed over both samples. Indeed, the Arrhenius plot in Fig. SI.4 yields an activation energy of 41.1 kJ mol^{-1} for the degreened sample, in agreement with the value reported by Paolucci *et al.*[15] (~35 kJ mol^{-1}) from AIMD simulations of $Cu^+(NH_3)_2$ diffusion. In contrast, the aged sample exhibits a greater activation energy of 58.0 kJ mol^{-1}, comparable to that reported by Deka *et al.*[41] using similar transient response experiments. These activation energies show that the OHC over the degreened

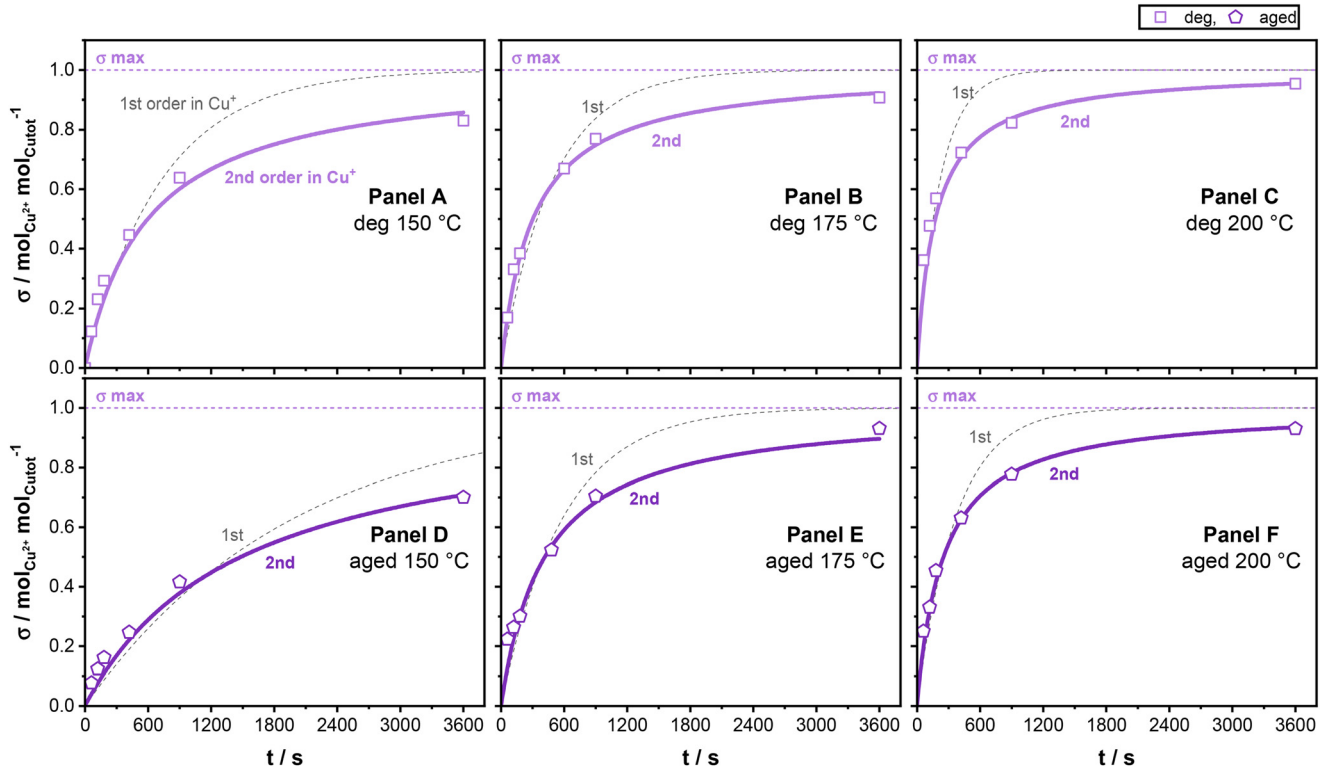

Fig. 3 Transient profiles of σ (Cu^{2+} fraction) *vs.* oxidation time during the OHC protocol on degreened and aged catalysts. Panels: A) deg 150 °C, B) deg 175 °C, C) deg 200 °C, D) aged 150 °C, E) aged 175 °C, F) aged 200 °C. Symbols: experimental data (squares for deg, pentagons for aged). Solid lines: 2nd order in Cu^+ model fit (used in this work). Gray dashed lines: 1st order in Cu^+ model fit. Feed: GHSV = 450 000 $cm^3\ h^{-1}\ g_{cat}^{-1}$ (STP); O_2 = 1.0% v/v and H_2O = 2.0% v/v in He.

catalyst is kinetically more favorable, whereas mild HTA makes the reaction less facile, requiring about 40% more energy to proceed. Overall, these results identify the OHC as the sole aging-sensitive component of the low-temperature redox cycle.

3.4. Combination of RHC and OHC in standard-SCR

To close the redox cycle, we herein proceed to combine RHC and OHC kinetics studied independently to analyze the standard-SCR and the related mild HTA effect. Fig. 4 shows the experimental data of the standard-SCR protocol over the degreened (panels A) and over the aged (panels B) samples at 200 °C. In addition, Fig. SI.5 and SI.6 show the corresponding results at 150 and 175 °C, respectively.

After the pre-reduction of the catalyst with NO + NH_3, we cofeed 8.0% v/v of O_2 to activate the standard-SCR activity, reaching steady-state conditions after a short transient, as shown in the first column of Fig. 4. At 200 °C, the NO conversions (X_{NO}) are equal to 75.9 and 68.8% for the degreened and the aged catalyst, respectively. As expected, and discussed in the Introduction, mild HTA reduced the X_{NO}. After two hours, the oxygen is once again removed to fully reduce the oxidized copper sites present during the steady-state standard-SCR reaction. This is depicted in the second column of Fig. 4 by the transient NO and N_2 profiles for the two samples. At 200 °C, we assess bed-average fractions of Cu^{2+} sites (σ_{ss}) at steady-state standard-SCR of 66.9 and 61.5%. As expected, mild HTA also decreased the Cu^{2+} fraction, and this is confirmed at all the temperatures investigated, as shown in Table 3, consistent with the slower OHC.

Table 2 OHC rate constants over the degreened and the aged samples at the three studied temperatures

k_{OHC}/s^{-1}	Degreened	Aged
150 °C	6.7×10^{-3}	2.8×10^{-3}
175 °C	13.2×10^{-3}	8.4×10^{-3}
200 °C	23.0×10^{-3}	15.9×10^{-3}

Based on the rate expressions eqn (2) and (3), and using the independently estimated rate constants, we proceed to simulate the standard-SCR activity. The model relies on equating the r_{RHC} and the r_{OHC} in order to compute X_{NO} and σ_{ss}. For the two catalyst samples, the solid lines in Fig. 4 show the model predictive simulations at 200 °C using the rate constants of Tables 1 and 2. A match of similar quality is illustrated in Fig. SI.5 and SI.6 for the data at 150 and 175 °C. Table 3 reports the model predictions of X_{NO} and σ_{ss}, compared to the experimental data. The mean absolute error for X_{NO} is 1.0%, while it is 0.2% for σ_{ss}. Clearly, our approach enables an accurate prediction of both the NO

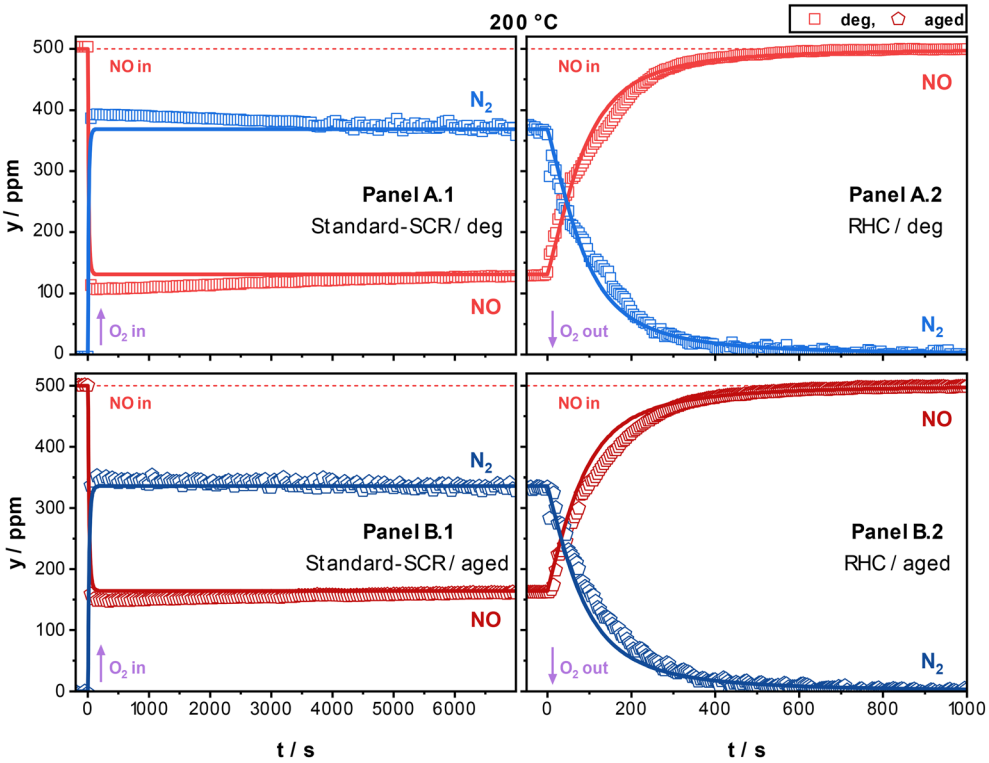

Fig. 4 NO and N_2 transient outlet concentration profiles during the standard-SCR protocol on degreened and aged samples at 200 °C. Panels: A) degreened, B) aged, 1) standard-SCR, 2) RHC following standard-SCR. Symbols: experimental data (red for NO, blue for N_2, squares for deg, pentagons for aged). Solid lines: model fit. Feed: GHSV = 450 000 $cm^3\ h^{-1}\ g_{cat}^{-1}$ (STP); NO = 500 ppm, NH_3 = 500 ppm, O_2 = 8.0–0.0% v/v and H_2O = 2.0% v/v in He.

conversion and the oxidized copper fraction at steady-state standard-SCR conditions. It is important to note that such an accurate match is achieved even though the OHC transient experiments were conducted at 1.0% v/v O_2, whereas the standard-SCR tests were carried out at 8.0%, which validates the linear dependence of r_{OHC} on oxygen concentration. Additionally, this confirms the reliability of the redox kinetic model in accurately describing the standard-SCR conditions over both the degreened and the aged samples. In particular, the model correctly predicts both the loss of low-T NO conversion and the decreased oxidized copper fraction under mild HTA solely *via* the inhibition of low-T OHC.

Table 3 Experimental and simulated NO conversion (X_{NO}) and bed-average oxidized Cu fraction (σ_{ss}) during steady-state standard-SCR over the degreened and the aged samples at the three studied temperatures: 150, 175, and 200 °C. Feed: GHSV = 450 000 $cm^3\ h^{-1}\ g_{cat}^{-1}$ (STP); NO = 500 ppm, NH_3 = 500 ppm, O_2 = 8.0% v/v and H_2O = 2.0% v/v in He. The experimental X_{NO} for degreened and aged samples are the same as shown in Fig. 1

	X_{NO}/%				σ_{ss}/%			
	Degreened		Aged		Degreened		Aged	
Steady-state standard-SCR	Exp.	*Model*	Exp.	*Model*	Exp.	*Model*	Exp.	*Model*
150 °C	33.7	*33.2*	24.9	*25.0*	55.4	*55.9*	47.7	*47.8*
175 °C	52.6	*51.8*	47.5	*46.8*	61.5	*61.5*	56.1	*56.3*
200 °C	75.9	*73.8*	68.8	*67.2*	66.9	*66.9*	61.5	*61.6*

Recently, Gao and coworkers[47] have proposed a complementary NO-active OHC route wherein NO and O_2 would re-oxidize the diamine Cu^+ species to form Cu^{2+} nitrates, subsequently decomposed by NO according to a fast-SCR pathway: this is essentially identical to the mechanism originally published by Janssens *et al.*[11] Using transient response methods like those herein applied, Gao and coworkers studied the Cu oxidation kinetics at very low temperatures (75–120 °C) over a single catalyst formulation, finding that the NO + O_2 OHC is faster than the O_2-only OHC under wet feed conditions (but not under dry feed conditions). By a complex extrapolation of these data to the temperatures of interest for SCR (185–230 °C), they concluded that account of such a parallel NO-active OHC pathway, although not the dominant oxidation mechanism, is necessary to improve the kinetic description of the standard-SCR reaction with respect to our model based on RHC + O_2-only OHC (NO silent). In our view, the results of the transient kinetic analysis herein reported (see Fig. 4 and Table 3) prove that, over the present industrial catalysts, a NO-silent OHC mechanism fully and predictively explains the steady-state standard-SCR activity both in terms of NO conversion and of bed-average Cu redox state, without the need for invoking additional Cu^+ oxidation routes. The contribution of a NO-to-nitrate OHC pathway, if any, is negligible in our experimental conditions: its addition to the redox model would only overparameterize it. This conclusion

is also in line with results previously published for other Cu-CHA catalysts with different Cu loadings and SAR.[16,45]

3.5. Oxygen-based recovery of activity

Since mild HTA affects only the OHC, we attempted to engineer a recovery of activity. Given the first order dependence on oxygen in eqn (3), a linear increment of the OHC rate is expected upon increasing the O_2 concentration. Considering that the rate constant decreases under mild HTA, to preserve the same OHC rate, the oxygen concentration must therefore be increased as follows:

$$y_{O_2} = \frac{k_{OHC}^{deg}}{k_{OHC}^{aged}} y_{O_2}^{deg} \quad (4)$$

To challenge this assumption, we first replicated the standard-SCR protocol at 4.0% v/v of O_2 over the degreened and aged samples at 200 °C. Fig. SI.7 shows the experimental results: for the degreened catalyst, we record a 62.0% NO conversion and 56.5% bed-average Cu^{2+} fraction, while for the aged catalyst, they are lowered to 53.7 and 52.0%, respectively. The redox model is once again able to predict the standard-SCR conditions also at this lower O_2 concentration, as visible from the solid lines in Fig. SI.7, which are superimposed on experimental data. These experiments can be used as a further validation of our model under conditions different from those of Fig. 4.

Then, we run an additional standard-SCR experiment over the aged sample, feeding a higher oxygen concentration. By using eqn (4) and the OHC rate constants at 200 °C in Table 2, the activity recovery should be achieved with y_{O_2} = 5.8% in the feed. Fig. SI.8 shows the results of this test, while the bar plot in Fig. 5 compares the results of the different experiments. With y_{O_2} = 5.8%, we achieve a full recovery of the activity: X_{NO} is 61.8% and σ_{ss} is 57.0%, *i.e.*, essentially identical to the degreened catalyst performances at 4.0% v/v of O_2.

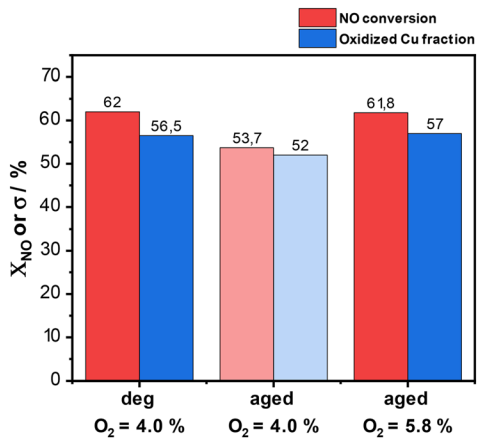

Fig. 5 NO conversion (X_{NO}, in red) and oxidized copper fraction (σ_{ss}, in blue) at steady-state standard-SCR over the degreened and aged samples at 200 °C and different O_2 concentrations (4.0 and 5.8% v/v). The highlighted columns represent the recovery of activity on the aged sample (with respect to the degreened) by increasing the O_2 partial pressure. Feed: GHSV = 450 000 $cm^3\ h^{-1}\ g_{cat}^{-1}$ (STP); NO = 500 ppm, NH_3 = 500 ppm, O_2 = 4.0/5.8% v/v and H_2O = 2.0% v/v in He.

Thus, by a simple increment of the O_2 concentration, we can fully restore the performance of the catalyst; also, we are able to predict this behavior by a simple two-reaction model. In production aftertreatment systems that use SCR catalysts, the upstream O_2 concentration can in principle be tuned by modifying the engine combustion strategy, allowing some adjustments in the oxygen level delivered to the SCR catalyst under low-temperature operating conditions. The model presented in this work can therefore be practically used as part of an onboard model-based control strategy to estimate the O_2 level that best compensates for hydrothermal aging and helps minimize system-level NOx emissions.

As a final note, we estimate the apparent kinetic orders of NO and oxygen in standard-SCR. Using the RHC and OHC rate equations with the fitted parameters, for both our investigated catalysts, we have computed the steady-state standard-SCR rate at different NO (100–2000 ppm) concentrations with fixed O_2 (8%), and then at different O_2 (1–20% v/v) concentrations with fixed NO (500 ppm). The results are plotted in Fig. SI.9A and B, respectively. Indeed, by differentiating the $\log_{10} r_{SCR}$, as in Fig. SI.10, we find fractional orders between 0 and 1 for both NO and O_2, confirming that the standard-SCR mechanism does not exhibit a clear RDS under the investigated conditions, with both RHC and OHC being kinetically relevant. We also show that the kinetic orders with respect to NO and O_2 vary significantly with operating conditions. As expected, at low NO and high O_2 concentrations, where the RDS is the RHC, the rate orders get close to those of the RHC rate (*i.e.*, 1st order in NO and 0th order in O_2), as in eqn (2). Instead, at high NO and low O_2, where the OHC becomes rate determining, we see a decrease in the NO order towards zero and an increase in the O_2 order, thus approaching eqn (3).

3.6. Combined effect of H_2O and HTA on RHC, OHC, and standard-SCR

The H_2O effect on the RHC and OHC kinetics was independently studied in previous works by some of us,[16,22] testing Cu-CHA samples varying in SAR. In this work, to check the combined effects of water and catalyst aging, we have run tests in dry-gas conditions for both RHC, OHC, and standard-SCR over the degreened and the aged samples. The data collected were compared with those obtained under wet feed conditions.

For the RHC, Fig. SI.11 shows the data at 150, 175, and 200 °C for both samples, while Table SI.3 reports the rate constants obtained from the model fit of these data. The RHC rate constants of both degreened and aged samples obtained under dry conditions are greater than the ones obtained in wet conditions under all the investigated conditions, in line with previous findings on different catalyst samples:[16,39] the presence of water inhibits the RHC

in high SAR samples due to entropy losses in presence of water being far greater than the enthalpic stabilization, as DFT calculations demonstrated.[48] Additionally, in dry-gas conditions, the mild HTA of the aged sample does not have a significant impact on the RHC rate constants, as shown by the Arrhenius plot in Fig. SI.12A.

For the standard-SCR, Table SI.4 reports steady-state NO conversions and oxidized copper fractions at three temperatures over the two catalysts. Small differences in NO conversion between the dry-gas and the wet conditions are observed, while the presence of H_2O clearly promotes the oxidation state of the catalyst. This is once again in line with the high SAR sample in Nasello *et al.*[16]

In this dry-gas case, following the procedure of our recent papers,[45,49] we have estimated the k_{OHC} based on the equivalence between RHC and OHC reaction rates (r_{RHC} = r_{OHC} = r_{SCR}) at steady-state standard-SCR. The estimates are reported in Table SI.5. Comparing them with the estimates obtained in wet conditions, we can clearly conclude that H_2O promotes the OHC both over the degreened and the aged sample. Furthermore, also in dry-gas conditions, the mild HTA inhibits only the OHC, as visible in the Arrhenius plot of Fig. SI.12B.

The H_2O inhibition of the RHC and the H_2O promotion of the OHC explain the apparently paradoxical observation of a marginal H_2O effect on the NO conversion at steady-state standard-SCR conditions, accompanied, however, by a promotion of the Cu oxidation state. As further validation of this concept, we have simulated the steady-state standard-SCR conversion at different feed NO feed concentrations (100–2000 ppm), both in dry and wet feed conditions, as shown in Fig. SI.13. These simulations are fully in line with the low-temperature data by Ottinger *et al.*,[50] who studied experimentally the H_2O effect on standard SCR at different NO feed concentrations. At low NO concentrations, the presence of water inhibits the NO conversion, while at high feed NO concentrations, a promotion is apparent. This complex behavior is nicely captured by our simple two-reaction model: at low y_{NO}^{in}, in fact, the RHC, which is indeed inhibited by H_2O, is slow and kinetically controls the standard-SCR activity; instead, at high y_{NO}^{in}, the OHC, which is promoted by H_2O, becomes rate controlling. Notably, this dual role of H_2O (RHC-inhibiting, OHC-promoting) remains valid also after mild HTA, and, most importantly, HTA consistently inhibits only the OHC, regardless of the presence or absence of H_2O.

4. Conclusions

Herein, we have investigated the effect of mild HTA on the low-temperature standard-SCR (150–200 °C) by applying transient response methods and kinetic modeling to study the RHC and the OHC independently, eventually combining them into the full redox cycle of the standard-SCR reaction.

– We have confirmed on a different set of catalysts that the low temperature reduction half-cycle is essentially unaffected by mild HTA, due to the hydrolysis reaction shifting Z_2Cu^{2+} to $ZCu^{2+}OH$. The second order kinetics in oxidized copper sites are confirmed. The activation energies of the degreened and aged samples are comparable.

– The novelty of this work lies in assessing the effect of mild HTA on the low temperature oxidation half-cycle. By transient kinetic analysis, we show that the OHC is slower over the aged sample in comparison to the degreened sample. In fact, both the oxidized copper fraction at SCR steady state and the OHC rate constant k_{OHC} are consistently smaller over the aged catalyst. The second order in the reduced copper sites is confirmed for the OHC rate, also in the case of the present industrial catalysts with high Cu loading. The activation energy of the aged sample is 40% higher than that of the degreened catalyst, indicating that the reaction is kinetically hindered by mild HTA.

– As in previous work, the combination of RHC and OHC kinetics to close the redox cycle of the low-temperature standard-SCR is again successful. Using the independent estimates of k_{RHC} and k_{OHC}, we predict the steady-state low-T NO conversion and bed-average oxidized Cu fraction over both the degreened and the aged industrial catalysts at all temperatures with a mean absolute error of only 0.6%. This rules out the need for complementary "NO-active" OHC pathways to describe the standard-SCR activity, as proposed in recent literature. Notably, this also implies that the inhibitory effect of mild HTA on the OHC is responsible for (and fully explains) the observed adverse HTA effect on the overall standard-SCR activity.

– Based on this evidence of a direct correlation between mild HTA and OHC and recalling that the OHC rate is first order in oxygen, we have engineered an oxygen-based recovery of activity. By increasing the oxygen partial pressure over the aged sample proportionally to the ratio of the k_{OHC} of the degreened and aged samples, we were able not only to restore the steady-state NO conversion but also the bed-average Cu^{2+} fraction to the same values of the degreened catalyst operated at the lower oxygen concentration.

– We have repeated the RHC and standard-SCR experiments in the absence of H_2O in the feed. In line with our previous work, we have confirmed that water has an inhibiting effect on the RHC (due to the high SAR) but a promoting effect on the OHC. This results in unchanged NO conversion but enhanced Cu oxidation state during steady-state standard-SCR over both the degreened and the aged samples when H_2O is included in the feed stream.

Overall, this study identifies OHC as the sole aging-sensitive step of the SCR redox mechanism. It also provides a simple but mechanistically grounded and, most of all, predictive kinetic framework linking HTA-induced Cu speciation changes to catalyst performance. The ability to fully restore the NH_3-SCR activity of an aged catalyst through oxygen management highlights the practical relevance of this understanding for designing more durable NH_3-SCR systems and improved control strategies of real exhaust aftertreatment systems.

Notably, the present work is focused on a specific Cu-SSZ-13 formulation, although representative of industrial NH_3-SCR catalysts. In principle, the observed selective inhibition of the OHC by mild HTA may depend on zeolite framework, Cu loading, and silica-to-alumina ratio, suggesting that further investigation of different Cu-zeolite systems is warranted to generalize the present conclusions.

Conflicts of interest

There are no conflicts of interest to declare.

Data availability

The data supporting this article are included in the main text and the supplementary information (SI). Additional data are not available. The SI contains catalyst characterization, Arrhenius plots, standard-SCR activity, conversion rates, and dry-gas data.

Supplementary information is available. See DOI: https://doi.org/10.1039/d6re00057f.

Acknowledgements

Cummins, Inc. has financially supported this study. We thank Professors William S. Epling and Christopher Paolucci for insightful discussions and valuable feedback. We also gratefully acknowledge MSc students Francesca Marra, Ricardo Esteban Pérez Hernández, and Andrea Giovanni Prodorutti for conducting part of the experimental work during their thesis projects at Politecnico di Milano.

References

1 A. Jeong, G. Lovison, A. Bussalleu, M. Cirach, P. Dadvand, K. de Hoogh, C. Flexeder, G. Hoek, M. Imboden, S. Karrasch, G. H. Koppelman, S. Kress, P. Ljungman, R. Majewska, G. Pershagen, R. Pickford, Y. Shen, R. C. H. Vermeulen, J. J. Vlaanderen, M. Vogli, K. Wolf, Z. Yu, E. Melén, A. Pac, A. Peters, T. Schikowski, M. Standl, U. Gehring and N. Probst-Hensch, Lung Function-Associated Exposome Profile in the Era of Climate Change: Pooled Analysis of 8 Population-Based European Cohorts within the EXPANSE Project, *Environ. Int.*, 2025, **196**, 109269, DOI: 10.1016/j.envint.2025.109269.

2 E. Mulholland, J. Miller, Y. Bernard, K. Lee and F. Rodríguez, The Role of NOx Emission Reductions in Euro 7/VII Vehicle Emission Standards to Reduce Adverse Health Impacts in the EU27 through 2050, *Transportation Engineering*, 2022, **9**, 100133, DOI: 10.1016/j.treng.2022.100133.

3 J. Leverett, W. H. Lie, M. H. A. Khan, Z. Ma, R. Daiyan and R. Amal, Navigating the Challenges of Global NO_x Emissions throughout the Energy Transition: State of Play and Outlook, *Sustainable Energy Fuels*, 2025, **9**(14), 3780–3790, DOI: 10.1039/D4SE01806K.

4 B. Zhao, S. X. Wang, H. Liu, J. Y. Xu, K. Fu, Z. Klimont, J. M. Hao, K. B. He, J. Cofala and M. Amann, NO_x Emissions in China: Historical Trends and Future Perspectives, *Atmos. Chem. Phys.*, 2013, **13**(19), 9869–9897, DOI: 10.5194/acp-13-9869-2013.

5 *Urea-SCR Technology for deNOx After Treatment of Diesel Exhausts*, ed. I. Nova and E. Tronconi, Fundamental and Applied Catalysis, Springer, New York, NY, 2014, DOI: 10.1007/978-1-4899-8071-7.

6 T. Selleri, A. D. Melas, A. Joshi, D. Manara, A. Perujo and R. Suarez-Bertoa, An Overview of Lean Exhaust deNOx Aftertreatment Technologies and NOx Emission Regulations in the European Union, *Catalysts*, 2021, **11**(3), 404, DOI: 10.3390/catal11030404.

7 J. H. Kwak, R. G. Tonkyn, D. H. Kim, J. Szanyi and C. H. F. Peden, Excellent Activity and Selectivity of Cu-SSZ-13 in the Selective Catalytic Reduction of NOx with NH_3, *J. Catal.*, 2010, **275**(2), 187–190, DOI: 10.1016/j.jcat.2010.07.031.

8 J. H. Kwak, D. Tran, S. D. Burton, J. Szanyi, J. H. Lee and C. H. F. Peden, Effects of Hydrothermal Aging on NH_3-SCR Reaction over Cu/Zeolites, *J. Catal.*, 2012, **287**, 203–209, DOI: 10.1016/j.jcat.2011.12.025.

9 J. Luo, H. An, K. Kamasamudram, N. Currier, A. Yezerets, T. Watkins and L. Allard, Impact of Accelerated Hydrothermal Aging on Structure and Performance of Cu-SSZ-13 SCR Catalysts, *SAE Int. J. Engines*, 2015, **08**(3), 1181–1186, DOI: 10.4271/2015-01-1022.

10 M. E. Azzoni, N. Usberti, A. Gjetja, I. Nova, E. Tronconi, R. Villamaina, M. P. Ruggeri, V. Georgieva, L. Mantarosie and J. Collier, Investigation of the Redox Properties of Fe-CHA Catalysts by Transient Response Methods, *Appl. Catal., A*, 2025, **707**, 120520, DOI: 10.1016/j.apcata.2025.120520.

11 T. V. W. Janssens, H. Falsig, L. F. Lundegaard, P. N. R. Vennestrøm, S. B. Rasmussen, P. G. Moses, F. Giordanino, E. Borfecchia, K. A. Lomachenko, C. Lamberti, S. Bordiga, A. Godiksen, S. Mossin and P. Beato, A Consistent Reaction Scheme for the Selective Catalytic Reduction of Nitrogen Oxides with Ammonia, *ACS Catal.*, 2015, **5**(5), 2832–2845, DOI: 10.1021/cs501673g.

12 M. Bendrich, A. Scheuer, R. E. Hayes and M. Votsmeier, Unified Mechanistic Model for Standard SCR, Fast SCR, and NO_2 SCR over a Copper Chabazite Catalyst, *Appl. Catal., B*, 2018, **222**, 76–87, DOI: 10.1016/j.apcatb.2017.09.069.

13 E. Borfecchia, P. Beato, S. Svelle, U. Olsbye, C. Lamberti and S. Bordiga, Cu-CHA – a Model System for Applied Selective Redox Catalysis, *Chem. Soc. Rev.*, 2018, **47**(22), 8097–8133, DOI: 10.1039/C8CS00373D.

14 D. J. Deka, R. Daya, A. Ladshaw, S. Y. Joshi and W. P. Partridge, A Transient-Response Methodology Based on Experiments and Modeling for Cu-Redox Half-Cycle Kinetic Analysis on a Cu-SSZ-13 SCR Catalyst, *Chem. Eng. J.*, 2022, **435**, 134219, DOI: 10.1016/j.cej.2021.134219.

15 C. Paolucci, I. Khurana, A. A. Parekh, S. Li, A. J. Shih, H. Li, J. R. D. Iorio, J. D. Albarracin-Caballero, A. Yezerets, J. T. Miller, W. N. Delgass, F. H. Ribeiro, W. F. Schneider and R. Gounder, Dynamic Multinuclear Sites Formed by Mobilized Copper Ions in NOx Selective Catalytic Reduction, *Science*, 2017, **357**(6354), 898–903, DOI: 10.1126/science.aan5630.

16 N. D. Nasello, U. Iacobone, N. Usberti, A. Gjetja, I. Nova, E. Tronconi, R. Villamaina, M. P. Ruggeri, D. Bounechada, A. P. E. York and J. Collier, Investigation of Low-Temperature OHC and RHC in NH_3 –SCR over Cu-CHA Catalysts: Effects of H_2 O and SAR, *ACS Catal.*, 2024, **14**(6), 4265–4276, DOI: 10.1021/acscatal.4c00118.

17 R. Daya, D. Trandal, U. Menon, D. J. Deka, W. P. Partridge and S. Y. Joshi, Kinetic Model for the Reduction of Cu^{II} Sites by NO + NH_3 and Reoxidation of NH_3 -Solvated Cu^{I} Sites by O_2 and NO in Cu-SSZ-13, *ACS Catal.*, 2022, **12**(11), 6418–6433, DOI: 10.1021/acscatal.2c01076.

18 C. Liu, H. Kubota, T. Amada, K. Kon, T. Toyao, Z. Maeno, K. Ueda, J. Ohyama, A. Satsuma, T. Tanigawa, N. Tsunoji, T. Sano and K. Shimizu, In Situ Spectroscopic Studies on the Redox Cycle of NH_3–SCR over Cu–CHA Zeolites, *ChemCatChem*, 2020, **12**(11), 3050–3059, DOI: 10.1002/cctc.202000024.

19 W. Hu, T. Selleri, F. Gramigni, E. Fenes, K. R. Rout, S. Liu, I. Nova, D. Chen, X. Gao and E. Tronconi, On the Redox Mechanism of Low-Temperature NH_3-SCR over Cu-CHA: A Combined Experimental and Theoretical Study of the Reduction Half Cycle, *Angew. Chem., Int. Ed.*, 2021, **60**(13), 7197–7204, DOI: 10.1002/anie.202014926.

20 F. Gramigni, N. D. Nasello, N. Usberti, U. Iacobone, T. Selleri, W. Hu, S. Liu, X. Gao, I. Nova and E. Tronconi, Transient Kinetic Analysis of Low-Temperature NH_3 -SCR over Cu-CHA Catalysts Reveals a Quadratic Dependence of Cu Reduction Rates on Cu^{II}, *ACS Catal.*, 2021, **11**(8), 4821–4831, DOI: 10.1021/acscatal.0c05362.

21 N. Usberti, F. Gramigni, N. D. Nasello, U. Iacobone, T. Selleri, W. Hu, S. Liu, X. Gao, I. Nova and E. Tronconi, An Experimental and Modelling Study of the Reactivity of Adsorbed NH_3 in the Low Temperature NH_3-SCR Reduction Half-Cycle over a Cu-CHA Catalyst, *Appl. Catal., B*, 2020, **279**, 119397, DOI: 10.1016/j.apcatb.2020.119397.

22 C. Negri, N. Usberti, G. Contaldo, M. Bracconi, I. Nova, M. Maestri and E. Tronconi, Quantitative Kinetic Insights from Operando-UV/Vis Spectroscopy: An Application to NH_3–SCR of NOx on Cu-CHA Catalysts, *Angew. Chem., Int. Ed.*, 2024, **63**(41), e202408328, DOI: 10.1002/anie.202408328.

23 G. Contaldo, C. Negri, N. Usberti, M. Bracconi, I. Nova, M. Maestri and E. Tronconi, The H_2O-Assisted Oxidation Half-Cycle of Low Temperature NH_3-SCR over Cu-CHA, 2026.

24 C. Paolucci, A. A. Parekh, I. Khurana, J. R. Di Iorio, H. Li, J. D. Albarracin Caballero, A. J. Shih, T. Anggara, W. N. Delgass, J. T. Miller, F. H. Ribeiro, R. Gounder and W. F. Schneider, Catalysis in a Cage: Condition-Dependent Speciation and Dynamics of Exchanged Cu Cations in SSZ-13 Zeolites, *J. Am. Chem. Soc.*, 2016, **138**(18), 6028–6048, DOI: 10.1021/jacs.6b02651.

25 F. Gao and J. Szanyi, On the Hydrothermal Stability of Cu/SSZ-13 SCR Catalysts, *Appl. Catal., A*, 2018, **560**, 185–194, DOI: 10.1016/j.apcata.2018.04.040.

26 R. Daya, S. Y. Joshi, J. Luo, R. K. Dadi, N. W. Currier and A. Yezerets, On Kinetic Modeling of Change in Active Sites upon Hydrothermal Aging of Cu-SSZ-13, *Appl. Catal., B*, 2020, **263**, 118368, DOI: 10.1016/j.apcatb.2019.118368.

27 R. Daya, D. Trandal, R. K. Dadi, H. Li, S. Y. Joshi, J. Luo, A. Kumar and A. Yezerets, Kinetics and Thermodynamics of Ammonia Solvation on Z_2Cu, ZCuOH and ZCu Sites in Cu-SSZ-13 – Implications for Hydrothermal Aging, *Appl. Catal., B*, 2021, **297**, 120444, DOI: 10.1016/j.apcatb.2021.120444.

28 C. T. Lao, J. Akroyd, N. Eaves, A. Smith, N. Morgan, D. Nurkowski, A. Bhave and M. Kraft, Investigation of the Impact of the Configuration of Exhaust After-Treatment System for Diesel Engines, *Appl. Energy*, 2020, **267**, 114844, DOI: 10.1016/j.apenergy.2020.114844.

29 Z. Zhang, R. Dong, G. Lan, T. Yuan and D. Tan, Diesel Particulate Filter Regeneration Mechanism of Modern Automobile Engines and Methods of Reducing PM Emissions: A Review, *Environ. Sci. Pollut. Res.*, 2023, **30**(14), 39338–39376, DOI: 10.1007/s11356-023-25579-4.

30 Y. Xi, C. Su, N. A. Ottinger and Z. G. Liu, Effects of Hydrothermal Aging on the Sulfur Poisoning of a Cu-SSZ-13 SCR Catalyst, *Appl. Catal., B*, 2021, **284**, 119749, DOI: 10.1016/j.apcatb.2020.119749.

31 S. Han, J. Cheng, C. Zheng, Q. Ye, S. Cheng, T. Kang and H. Dai, Effect of Si/Al Ratio on Catalytic Performance of Hydrothermally Aged Cu-SSZ-13 for the NH_3-SCR of NO in Simulated Diesel Exhaust, *Appl. Surf. Sci.*, 2017, **419**, 382–392, DOI: 10.1016/j.apsusc.2017.04.198.

32 J. Luo, D. Wang, A. Kumar, J. Li, K. Kamasamudram, N. Currier and A. Yezerets, Identification of Two Types of Cu Sites in Cu/SSZ-13 and Their Unique Responses to Hydrothermal Aging and Sulfur Poisoning, *Catal. Today*, 2016, **267**, 3–9, DOI: 10.1016/j.cattod.2015.12.002.

33 U. Iacobone, N. D. Nasello, I. Nova, E. Tronconi, R. Daya, H. An and U. Menon, Assessing Cu2+ Active Sites Evolution on Cu-SSZ-13 NH_3-SCR Catalysts during Hydrothermal Aging: A Transient Response Approach, *Appl. Catal. B Environ. Energy*, 2024, **351**, 123989, DOI: 10.1016/j.apcatb.2024.123989.

34 F. Gao, N. M. Washton, Y. Wang, M. Kollár, J. Szanyi and C. H. F. Peden, Effects of Si/Al Ratio on Cu/SSZ-13 NH_3-SCR Catalysts: Implications for the Active Cu Species and the Roles of Brønsted Acidity, *J. Catal.*, 2015, **331**, 25–38, DOI: 10.1016/j.jcat.2015.08.004.

35 M. Wenig, R. Khare, A. Jentys and J. A. Lercher, Hydrothermal Stability of Active Sites in Cu-Exchanged Small-Pore Zeolites for the Selective Catalytic Reduction of NOx, *Angew. Chem., Int. Ed.*, 2025, **64**(5), e202416954, DOI: 10.1002/anie.202416954.

36 J. Zhang, W. Liu, Q. Wang, F. Ning, Q. He, G. Li, C. Liu, Z. Li and H. Peng, Effects of Cu Species in Cu-SSZ-13 Zeolites on the Performance of NOx Reduction Reactions, *Sep. Purif. Technol.*, 2024, **346**, 127544, DOI: 10.1016/j.seppur.2024.127544.

37 D. J. Deka, G. Lee, K. G. Rappé, E. Walter, J. Szanyi and Y. Wang, Influence of H_2 -ICE Specific Exhaust Conditions on the Activity and Stability of Cu-SSZ-13 deNO_x Catalysts, *Catal. Sci. Technol.*, 2025, **15**(11), 3256–3261, DOI: 10.1039/D5CY00095E.

38 T. Zheleznyak, P. Kočí and W. Epling, Impact of Mild Hydrothermal Aging on Kinetics of NH_3, NO, SO_2 and CO Oxidation Reactions on Cu/SSZ-13 Catalyst, *Chem. Eng. J.*, 2024, **489**, 151194, DOI: 10.1016/j.cej.2024.151194.

39 N. D. Nasello, U. Iacobone, A. Gjetja, I. Nova, E. Tronconi, R. Daya, L. Wei, H. An and K. Kamasamudram, Transient Kinetic Analysis of the Standard SCR Reduction Half Cycle on Cu-SSZ-13 Catalysts: Roles of Temperature, Hydrothermal Aging and H2O Feed Content, *Appl. Catal. B Environ. Energy*, 2024, **358**, 124360, DOI: 10.1016/j.apcatb.2024.124360.

40 W. Hu, U. Iacobone, F. Gramigni, Y. Zhang, X. Wang, S. Liu, C. Zheng, I. Nova, X. Gao and E. Tronconi, Unraveling the Hydrolysis of Z_2 Cu^{2+} to ZCu^{2+} $(OH)^-$ and Its Consequences for the Low-Temperature Selective Catalytic Reduction of NO on Cu-CHA Catalysts, *ACS Catal.*, 2021, **11**(18), 11616–11625, DOI: 10.1021/acscatal.1c02761.

41 D. J. Deka, R. Daya, A. Ladshaw, D. Trandal, S. Y. Joshi and W. P. Partridge, Assessing Impact of Real-World Aging on Cu-Redox Half Cycles of a Cu-SSZ-13 SCR Catalyst via Transient Response Measurements and Kinetic Modeling, *Appl. Catal., B*, 2022, **309**, 121233, DOI: 10.1016/j.apcatb.2022.121233.

42 A. Grossale, I. Nova, E. Tronconi, D. Chatterjee and M. Weibel, The Chemistry of the NO/NO_2–NH_3 "Fast" SCR Reaction over Fe-ZSM5 Investigated by Transient Reaction Analysis, *J. Catal.*, 2008, **256**(2), 312–322, DOI: 10.1016/j.jcat.2008.03.027.

43 M. Colombo, I. Nova and E. Tronconi, Detailed Kinetic Modeling of the NH_3–NO/NO_2 SCR Reactions over a Commercial Cu-Zeolite Catalyst for Diesel Exhausts after Treatment, *Catal. Today*, 2012, **197**(1), 243–255, DOI: 10.1016/j.cattod.2012.09.002.

44 R. Villamaina, S. Liu, I. Nova, E. Tronconi, M. P. Ruggeri, J. Collier, A. York and D. Thompsett, Speciation of Cu Cations in Cu-CHA Catalysts for NH_3 -SCR: Effects of SiO_2 /AlO_3 Ratio and Cu-Loading Investigated by Transient Response Methods, *ACS Catal.*, 2019, **9**(10), 8916–8927, DOI: 10.1021/acscatal.9b02578.

45 N. Usberti, R. Resmini, A. Gjetja, M. E. Azzoni, I. Nova, E. Tronconi, R. Villamaina, M. P. Ruggeri, D. Bounechada, A. P. E. York and J. Collier, Standard NH_3-SCR and N_2O Formation Kinetics over Cu-CHA Monolith Catalysts: Transient and Steady-State Redox Models, *Chem. Eng. J.*, 2026, **529**, 172622, DOI: 10.1016/j.cej.2026.172622.

46 D. Yao, B. Liu, F. Wu, Y. Li, X. Hu, W. Jin and X. Wang, N_2O Formation Mechanism During Low-Temperature NH_3-SCR over Cu-SSZ-13 Catalysts with Different Cu Loadings, *Ind. Eng. Chem. Res.*, 2021, **60**(28), 10083–10093, DOI: 10.1021/acs.iecr.1c01514.

47 S. Wang, M. Shen, G. Tian, Z. Liu, G. Shen, Y. Wang, X. Li, L. Jia, W. Li, X. Li and F. Gao, Reassessing the Oxidant Requirements in the Oxidation Half Cycle of Low-Temperature NH_3-SCR on Cu-SSZ-13 Catalysts, *Chem. Eng. J.*, 2026, **530**, 173427, DOI: 10.1016/j.cej.2026.173427.

48 G. Contaldo, M. Ferri, C. Negri, I. Nova, M. Maestri and E. Tronconi, First-Principles Assessment of the Role of Water in the Reduction Half Cycle of Low-Temperature NH_3-SCR over Cu-CHA, *ChemCatChem*, 2023, **15**(20), e202300673, DOI: 10.1002/cctc.202300673.

49 P. De Angeli, A. Lanza, N. Usberti, I. Nova, E. Tronconi, R. Villamaina, M. P. Ruggeri, D. Bounechada, A. York, T. Hlavatý and P. Kočí, A Simple Analytical Equation to Assess the Probe Effect on Spaci-Ms Data: Computational and Experimental Validation for the Redox Kinetics of Low-T NH_3-SCR Over a Cu-CHA Monolith Catalyst, *Chem. Eng. J.*, 2025, **512**, 162101, DOI: 10.1016/j.cej.2025.162101.

50 N. Ottinger, Y. Xi, C. Keturakis and Z. G. Liu, Impact of Water Vapor on the Performance of a Cu-SSZ-13 Catalyst under Simulated Diesel Exhaust Conditions, *SAE Int. J. Adv. Curr. Pract. Mobil.*, 2021, **3**(6), 2872–2877, DOI: 10.4271/2021-01-0577.

